

Available online at www.sciencedirect.com**ScienceDirect**

Energy Procedia 79 (2015) 612 – 619

Energy
Procedia

2015 International Conference on Alternative Energy in Developing Countries and
Emerging Economies

Effects of the Geometry of the Air Flowfield on the Performance of an Open-Cathode PEMFC – Transient Load Operation

Suangrat Kiattamrong^{a*,b}, Angkee Sripakagorn^{a,b},

^a*Department of Mechanical Engineering, Faculty of Engineering, Chulalongkorn University, Bangkok, Thailand*

^b*Fuel Cell Research Group, Chulalongkorn University, Bangkok, Thailand*

Abstract

The single-cell open-cathode PEMFC was fabricated with 100-cm² activation area to study the influence of the geometry of the air flowfield on the performance. Six cathode flowfield plates with different channel configurations were tested and compared under limited amount of air supplied. The transient load is applied with sinusoidal variations representative of the automotive load profile. The results were compared in the form of the hysteresis loop on the polarization curve. The effect of mass transfer loss was found at the high current density region. The flowfield with high aspect ratio gave a better performance. On the other hand, the flow area played no significant effect on the performance.

© 2015 The Authors. Published by Elsevier Ltd. This is an open access article under the CC BY-NC-ND license (<http://creativecommons.org/licenses/by-nc-nd/4.0/>).

Peer-review under responsibility of the Organizing Committee of 2015 AEDCEE

Keywords: PEMFC; transient load; open-cathode; flow channel

1. Introduction

Due to the increasing concern on the energy security and climate situation, electric vehicle is being developed continually to replace the conventional automobiles for the past few decades.

Recently, fuel cell vehicle is proposed as another promising option. A proton exchange membrane fuel cell (PEMFC) is outstanding among the other fuel cells technologies which limits in the operating

* Corresponding author. Tel.: +668-4527-1091.

E-mail address: Suangrat.K@gmail.com.

temperature and heavy weight. The performance and the durability of the PEMFC keep improving if not for its high capital cost that put paramount constraint against its future in the automotive application [1].

To eradicate this pitfall, the open-cathode PEMFC was introduced [2]. The design goals are to increase the system efficiency and reduce the auxiliary system cost. Similar to the typical PEMFC, previous studies pointed out that air channel configuration plays a crucial role to the performance for the open-cathode PEMFC [3-6]. The PEMFC with the wider air channel behaves better due to its high rate of the dissolved air onto the MEAs [3-4] and the deeper channel can dissipate more heat from the electrical generation [4], which are in accordance with the results from the typical PEMFC [5-6]. It should be noted, however, that in these works, the variation of the channel shape had been done without the concern that the variation also changed the total flow area. Furthermore, many channel configurations were studied without the concern on the mechanical stress and the lack of the reactant uniformity leading to lower the fuel cell efficiency and short the fuel cell life [9-12]. Most of the studies are also concentrated on the natural-convection type of open-cathode design whose performance is limited because of the insufficient supplied air [7-8]. In comparison, the study on the forced-air type is rather limited.

This study attempted to illustrate the influence of the geometry of the air flowfield on the performance of the forced-air type open-cathode PEMFC in the limited but sufficient air supply condition for the sake of the compact unit. The specimens were tested under the transient load to reflect automotive operating conditions. The results were discussed comparing with the results from the steady load.

Nomenclature

Symbols

f	friction loss coefficient
i	current density ($A\ cm^{-2}$)
I	current (A)
K	minor loss coefficient
L	length of the flow channel (m)
HHV	higher heating value ($J\ kg^{-1}$)
\dot{m}	mass flow rate ($kg\ s^{-1}$)
N_{cell}	numbers of the fuel cells in stack
Δp	pressure drop ($N\ m^{-2}$)
P	power (W)
R	resistance (Ω)
Re	Reynolds number
T	temperature (K)
v	air velocity ($m\ s^{-1}$)
V	voltage (V)
ΔV	voltage loss (V)
W	width of the flow channel (m)
D	depth of the flow channel (m)
λ	air stoichiometry
ρ	density ($kg\ m^{-3}$)
M	molecular weight ($kg\ mol^{-1}$)
x	mole ratio
$E_{(T,P)}$	thermodynamic reversible potential
ΔH	change in enthalpy ($J\ mol^{-1}$)
n	number of transferred electron per mole
ΔS	change in entropy

Subscripts

air	air
H_2	hydrogen
$cool$	cooling
in	inlet
out	outlet
$cell$	cell
$stack$	fuel cell stack
$prod$	product of reaction
$react$	reactant of reaction
cnv	convection
rad	radiation
fc	fuel cell
act	activation loss
ohm	Ohmic loss
mt	mass transfer loss

F	Faraday's constant
a	activity at inlet condition
ν_i	corresponding stoichiometric coefficient
i_L	limiting current density

2. Experimental Methodology

2.1 Test Unit

The single-cell open-cathode PEMFC was fabricated as the test unit. The active area of the membrane electrolyte membrane (MEA) was 100 cm². This 5-layer MEA was for utilize with hydrogen and air. The membrane was Nafion® 112 and coated with 410- μ m thickness of carbon cloth gas diffusion layer (GDL). The platinum content and loading were 60 wt% and 0,5 mg/cm², respectively. The silicone seals were used as the gasket to prevent the reactant leakage. Its components and assembly was in Fig. 1.

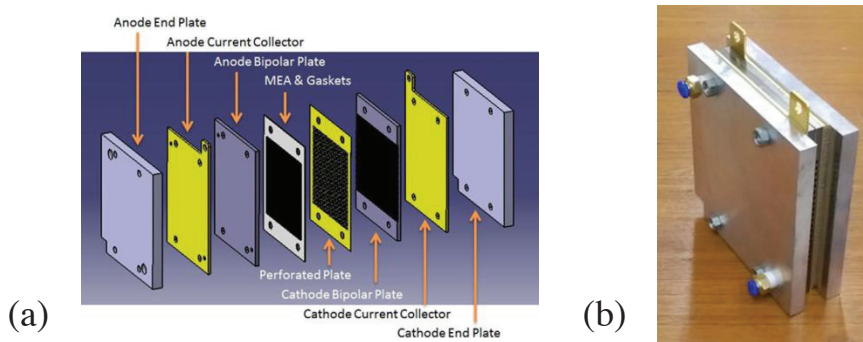




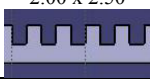
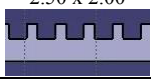
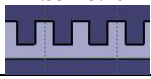
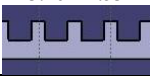
Fig. 1. (a) The components and assembly of the test unit; (b) the test unit

The perforated plate was specially prepared and placed between the cathode bipolar plate and MEA to protect MEA from the damage caused by the different pressure between the air and the hydrogen channels. The 60 degree-staggered circular holes were fabricated on the 0.4 mm thin copper plate. For low contact resistance, the perforated plate was coated with gold. The clamping pressure was set at 1 MPa.

The focus of this study is on the flowfield configurations of the bipolar plates. The bipolar plates were made of the graphite plates. Six cathode bipolar plates were prepared with the different straight air flowfield configurations; two aspect ratios and three flow areas (described in Table 1). For the present study, the aspect ratio is defined as the ratio of the width divided by the depth. The parallel-serpentine flowfield was patterned on the anode bipolar plate. The hydrogen flow was designed to be dead-end mode.

The current collectors were the gold-plating machined copper plates. The thickness of the copper plates was 3 mm. There were the connector ports to link to the electronic load and the data acquisition (DAQ). The endplates were fabricated from the aluminum 7075 plates. The 6 mm inlet and outlet ports were fitted on the anode side for the hydrogen flow to the anode bipolar plate.

Table 1. Air flowfield configurations

Flow Area (mm ²)	Aspect Ratio		No. of Channels
	0.80	1.25	
2	1.26 x 1.58 	1.58 x 1.26 	40
5	2.00 x 2.50 	2.50 x 2.00 	25
8	2.53 x 3.16 	3.16 x 2.53 	20

2.2 Forced-air supply

To properly assess the influence of the air flowfield geometry in the forced-air type unit, the air supply is selected to precisely feed sufficient air to the test cell for the electrochemical process and the transfer of heat produced from the process. The amount of air required by the fan unit is calculated from [13]

$$\dot{m}_{air,in} = \frac{\lambda M_{air} N_{cell} I_{stack}}{4xO_2 F} \quad (1)$$

$$\dot{m}_{H_2,in} = \frac{M_{H_2} N_{cell} I_{stack}}{2F} \quad (2)$$

$$\dot{m}_{air,cool} = \frac{\dot{m}_{H_2,in} HHV_{H_2} - P_{stack} - (\dot{Q}_{cvt} + \dot{Q}_{rad})}{C_{p,air}(T_{cool,out} - T_{cool,in})} \quad (3)$$

To support the desired maximum output of 30 A or 300 mA/cm² at 0.5 V, the fan unit was also needed to generate the sufficient level of pressure against the pressure drop inside the channel [13]

$$\Delta p = \sum K \rho \frac{v^2}{2} + \sum f \frac{L}{D_h} \rho \frac{v^2}{2} \quad (4)$$

where

$$f = \frac{55 + 41.5e^{-\frac{3.4}{W/D}}}{Re} \quad (5)$$

The pressure drop in the air channel was determined, plotted and compared with the characteristic curves of the fans as shown in Fig. 2. Finally, three fans were chosen, such as, SUNON MC25100V1, MC17080V1 and MC17080V2 supplied by MMMM. The MC25100V1 model for the 2 mm²-channel can precisely supply the evaluated air flow rate, while the MC17080V1 and MC17080V2 models for 5 and 8 mm²-channels can supply at slightly higher flow rate than the requirement.

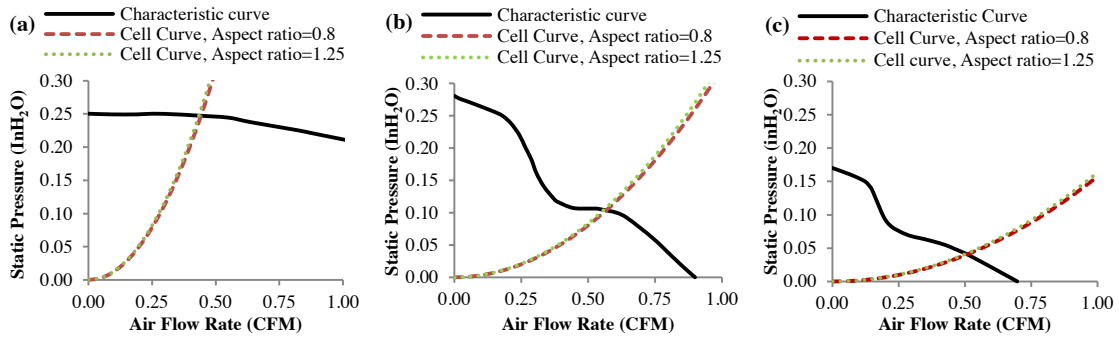


Fig. 2. The operating point of (a) SUNON MC25100V1 for the 2 mm²-air channel (b) MC17080V1 for the 5 mm²-air channel (c) MC17080V2 for the 8 mm²-air channel

2.3 Test Rig

The test rig (in Fig. 3) was separated into three parts; the single-cell fuel cell unit, the air tunnel, and the controlling unit. From the fuel cell unit, the current collectors were wired to the DAQ and electronic load. The hydrogen inlet and outlet lines were connected to their ports on the endplate. The air tunnel part was movable to easily adjust to fit the fuel cell unit. The fan was installed on the square end of the air tunnel. The power supply for the fan was from the 5 VDC supply on the controlling unit. The controlling unit also contains the purging valve and its circuit for manual operation. The 12 VDC supply from the external source feeds the controlling unit. The hydrogen input valve was also on this unit. The hydrogen pressure from the reservoir was adjusted to 2 psi.

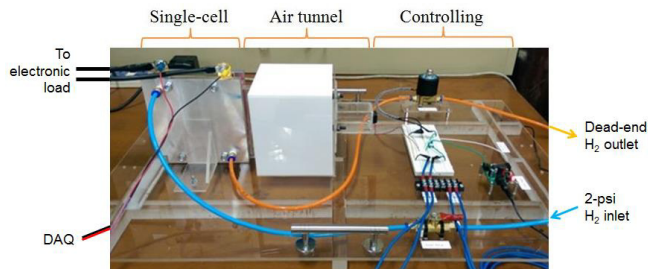


Fig. 3. The test rig

2.4 Experimental Procedure

As the previous work was focused on the steady load operation [14], the present experiment was conducted to the single-cell test unit under the transient load. The sinusoidal load variations with the amplitude of 15 A, the range within 0 – 30 A, with the frequency at 0.1 Hz were applied as the load profile. The ambient condition was specified at the temperature of 25°C and the relative humidity within

60-70%. The results that represent each test unit were obtained after the operation of the open-cathode PEMFC arrived at the quasi-steady state.

3. Results and Discussion

To put the present results in perspective, the previous results [14] are recalled in Fig.5. The steady-state test on the same unit revealed the drop in the performance at the high current density. In a fuel cell, the loss in the cell voltage was determined by

$$V_{fc} = E_{(T,P)} - \Delta V_{act} - \Delta V_{ohm} - \Delta V_{mt} \tag{6}$$

when

$$E_{(T,P)} = -\left(\frac{\Delta H}{nF} - \frac{T\Delta S}{nF}\right) - \frac{RT}{nF} \ln\left(\frac{\prod a_{prod}^{v_i}}{\prod a_{react}^{v_i}}\right) \tag{7}$$

$$\Delta V_{act} = \frac{RT}{\alpha nF} \ln\left(\frac{i}{i_0}\right) \tag{8}$$

$$\Delta V_{ohm} = i \cdot R_{ohm} \tag{9}$$

$$\Delta V_{mt} = \frac{RT}{\alpha nF} \ln\left(\frac{i_L}{i_L - i}\right) \tag{10}$$

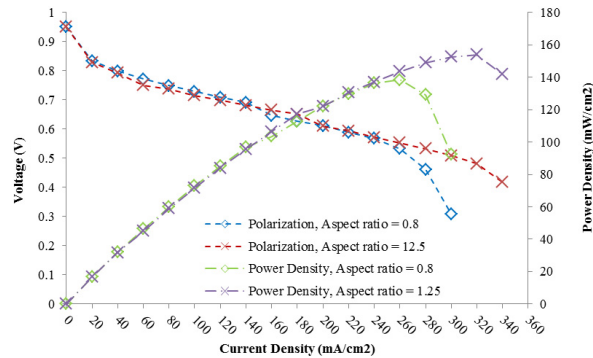


Fig. 4. The results from the steady load operation [14]

The mass transfer loss is important in this high current density region [15]. Consequently, the behavior illustrated by Fig. 5 showed the importance of the air dissolvability on the MEAs in the steady operation of the open-cathode PEMFC.

Under the transient load operation, the hysteresis loops appeared instead of the polarization curves as shown in Fig. 4. For all air flow field configurations, test units can operate at the desired point. There was, however, the significant different performance from the test unit with the different aspect ratios. The test unit with the higher aspect ratio consistently performed better as its hysteresis loop was always above the other. The difference is more pronounced at the high current density region. Under the dynamic

operation, the wide air channel was suggested to be more preferable than the narrow channel in the typical PEMFC due to the same reason [16]. A further notice at low current density region showed that the 5 mm²-and-aspect ratio 0.80 channel performed at a slightly lower voltage compared to the other cases. This is despite the fact that all test units performed quite similarly at this low current density region in the steady load operation. It was observed visually later on that, for this particular case, the voltage drop is due to the water flooding.

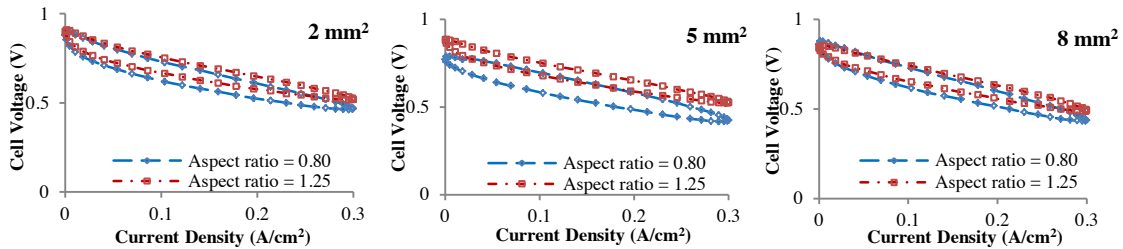


Fig. 5. Comparison of the behaviour of the test unit with the constant flow area and different aspect ratios.

Figure 6 illustrated on the influence of the flow area on the performance under transient operation. Like the previous results in steady-state conditions, the flow area played no effect on the fuel cell performance in the case that the sufficient and comparable air flow rate was forced through the cathode channels. There was no difference between the hysteresis loops from the test unit with different flow area as seen in Fig. 6. This also confirmed the conclusion on the previous study that the performance of the open-cathode PEMFC was strongly consistent with the air stoichiometry.

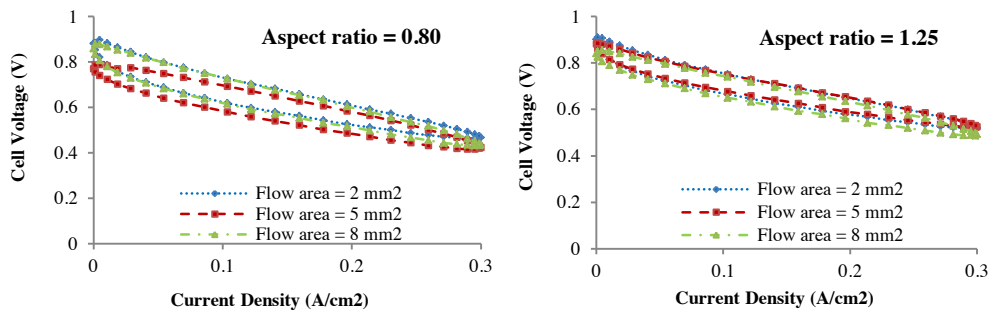


Fig. 6. Comparison of the behaviour of the test unit with the constant aspect ratio and different flow areas.

4. Conclusion

The open-cathode PEMFC was fabricated to study on the effects of different configurations of the cathode channel. Six different sets of the aspect ratio (width/depth) and the flow area are tested. All test units were supplied by the predetermined amount of air flow rate calculated to meet the electrochemical and thermal requirements. The results from the transient operation confirmed the results from the steady operation. The flow area does not have the strong influence on the fuel cell performance when the precise air flow rate is supplied. The open-cathode PEMFC tends to work better with the higher aspect ratio due

to the better dissolvability of the air on the MEAs. The aspect ratio of the air channel should not be too high, however, to avoid the issue of the mechanical stress.

Acknowledgements

This study was supported by Chula Unisearch, Special Task Force for Activating Research (STAR) and Fuel Cell Research Group of Chulalongkorn University.

References

- [1] Offer GJ et al. Comparative analysis of battery electric, hydrogen fuel cell and hybrid vehicles in a future sustainable road transport system, *Energy Policy* 2010; **38**: 24-29.
- [2] Squadrito G, et al. Polymer electrolyte fuel cell stack research and development, *International Journal of Hydrogen Energy* 2008; **33**: 1941-1946.
- [3] Kumar PK, Kolar AK. Effect of cathode channel dimensions on the performance of an air-breathing PEM fuel cell, *International Journal of Thermal Sciences* 2010; **49**: 844-857.
- [4] Tabe Y et al. Effect of cathode separator structure on performance characteristics of free-breathing PEMFCs, *Journal of Power Sources* 2006; **162**: 58-65.
- [5] Shimpalee S, Zee JWV. Numerical studies on rib&channel dimension of flow-field on PEMFC performance", *International Journal of Hydrogen Energy* 2007; **32**: 842 – 856.
- [6] Choi KS et al. Numerical studies on the geometrical characterization of serpentine flow-field for efficient PEMFC, *International Journal of Hydrogen Energy* 2011; **36**: 1613-1627.
- [7] Paquin M, Frechette LG. Understanding cathode flooding and dry-out for water management in air breathing PEM fuel cells, *Journal of Power Sources* 2008; **180**: 440-451.
- [8] Santa Rosa DT et al. High performance PEMFC stack with open-cathode at ambient pressure and temperature conditions, *International Journal of Hydrogen Energy* 2007; **32**: 4350-4357.
- [9] Wang XD et al. Numerical study on channel size effect for proton exchange membrane fuel cell with serpentine flow field, *Energy Conversion and Management* 2010; **51**: 959-968.
- [10] Zhang J et al. *PEM Fuel Cell Testing and Diagnosis*, 1st ed. Elsevier Academic Press; 2013.
- [11] Nitta I et al. Contact resistance between gas diffusion layer and catalyst layer of PEM fuel cell", *Electrochemistry Communications* 2008; **10**: 47-51.
- [12] Hottinen T, Himanen O. PEMFC temperature distribution caused by inhomogeneous compression of GDL, *Electrochemistry Communications* 2007; **9**: 1047-1052.
- [13] Barbir F. *PEM Fuel Cells: Theory and Practice*, 1st ed. Elsevier Academic Press; 2005.
- [14] Kiattamrong S, Sripakagorn A. Effects of the Geometry of the Air Flowfield on the Performance of an Open-Cathode PEMFC, *Proceedings of 5th international Conference on Sustainable Energy and Environment (SEE2014)* 2014: 408-413.
- [15] Husar A et al. Experimental characterization methodology for the identification of voltage losses of PEMFC: Applied to an open cathode stack, *International Journal of Hydrogen Energy* 2010; **37**: 7309-7315.
- [16] Shimpalee S, Zee JWV. Numerical studies on rib&channel dimension of flow-field on PEMFC performance, *International Journal of Hydrogen Energy* 2007; **32**: 842-856.